DOI: 10.1002/ejic.200600942

Mixed-Metal Dawson Sandwich Complexes: Synthesis, Spectroscopic Characterization and Electrochemical Behaviour of $Na_{16}[M^{II}Co_3(H_2O)_2(P_2W_{15}O_{56})_2]$ (M = Mn, Co, Ni, Zn and Cd)

Laurent Ruhlmann,*[a] Claire Costa-Coquelard,[a] Jacqueline Canny,[b] and René Thouvenot*[b]

Keywords: Dawson complexes / Paramagnetic ^{31}P NMR spectroscopy / Electrochemistry

Mixed-metal Dawson sandwich complexes $[MCo_3(H_2O)_2(P_2W_{15}O_{56})_2]^{16-}$ (represented as $\{MCo_3P_4W_{30}\}$) have been synthesized by the reaction of M^{2+} (where M = Mn, Co, Ni, Zn and Cd) with the "lacunary" sandwich complex αβ-$[NaCo_3(H_2O)_2(P_2W_{15}O_{56})_2]^{17-}$ (represented as $\{NaCo_3P_4W_{30}\}$): $[NaCo_3(H_2O)_2(P_2W_{15}O_{56})_2]^{17-} + M^{2+} \rightarrow [MCo_3(H_2O)_2(P_2W_{15}O_{56})_2]^{16-} + Na^+$. The $\{MCo_3P_4W_{30}\}$ species were characterized by IR spectroscopy, elemental analysis and ^{31}P solution NMR spectroscopy. The electrochemical behaviour of these mixed-metal sandwich complexes was investigated in aqueous solution and compared with that of ββ-$[Co_4(H_2O)_2(P_2W_{15}O_{56})_2]^{16-}$ (represented as ββ-$\{Co_4P_4W_{30}\}$) and $\{NaCo_3P_4W_{30}\}$.

Introduction

Polyoxometalates (POMs) and their transition-metal-substituted derivatives are metal–oxygen anionic clusters with applications in fields as diverse as magnetochemistry, medicine and catalysis.[1–4]

All investigations centred around this large and growing class of clusters required previous knowledge of their precise composition and structure; therefore, the continuing development of rational methods for the systematic modification of POM systems remains very important.

It is well known that the reaction of the trivacant Dawson anion α-$[P_2W_{15}O_{56}]^{12-}$ with transition-metal cations yields sandwich complexes $[M_4(H_2O)_2(P_2W_{15}O_{56})_2]^{16-}$ (M^{2+} = Mn^{2+}, Co^{2+}, Ni^{2+}, Zn^{2+} and Cd^{2+}), in which a sheet of four M atoms (two internal and two external) is sandwiched between two $\{P_2W_{15}\}$ subunits.[5] For all Dawson, tetranuclear, sandwich complexes characterized by X-ray diffraction, the "classical" ββ configuration is observed with β connectivities between both trivacant $\{P_2W_{15}\}$ units and the central M_4 tetrad[5c,5e,5f,5h] (Figure 1a). This type of arrangement leads to a molecular anion with C_{2h} symmetry in which the two $\{P_2W_{15}\}$ moieties are equivalent.

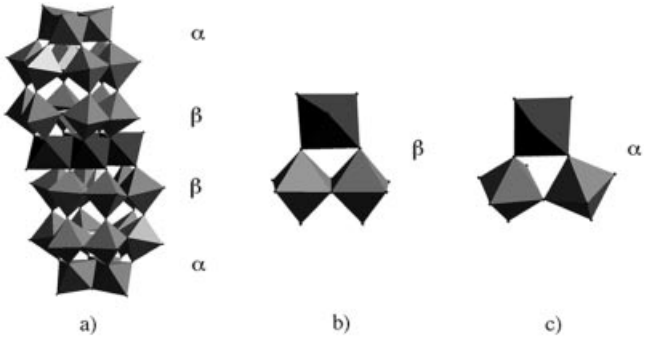

Figure 1. Polyhedral representation of the (a) αββα-$\{M_4P_4W_{30}\}$ sandwich structure, and of the (b) β and (c) α junctions.

The β junction implies a connection between one internal MO_6 octahedron and one dimeric W_2O_{10} unit (Figure 1b), whereas for the α junction, this internal MO_6 octahedron is connected to two dimeric W_2O_{10} units (Figure 1c).[6]

In the case of cobalt complexes, we previously reported that the synthesis in neutral solution leads to a mixture of symmetrical and unsymmetrical complexes as shown by ^{31}P NMR spectroscopy.[7a] One reasonable hypothesis for the structure of the dissymmetrical $\{Co_4P_4W_{30}\}$ species is that it presents both types of junction, α and β, between the two $\{P_2W_{15}\}$ units and the central Co_4 sheet.

[a] Laboratoire de Chimie Physique,
UMR CNRS 8000, Université Paris-Sud 11,
Bâtiment 350, 91405 Orsay Cedex, France
Fax: +33-1-69-15-43-28
E-mail: laurent.ruhlmann@lcp.u-psud.fr
[b] Laboratoire de Chimie Inorganique et Matériaux Moléculaires,
UMR CNRS 7071, Université Pierre et Marie Curie – Paris6,
Institut de Chimie Moléculaire FR 2769,
Case Courrier 42, 4, Place Jussieu, 75252 Paris Cedex 05, France
Fax: +33-1-44-27-38-41
E-mail: rth@ccr.jussieu.fr
Supporting information for this article is available on the WWW under http://www.eurjic.org or from the author.

Dinuclear and trinuclear sandwich complexes $[Na_2M_2(H_2O)_2(P_2W_{15}O_{56})_2]^{n-}$ and $[NaM_3(H_2O)_2(P_2W_{15}O_{56})_2]^{m-}$ (M^{2+} = Co^{2+}, n = 18, m = 17 and M^{3+} = Fe^{3+}, n = 16, m = 14) have also been obtained.[7b,7c,8,9]

For the diiron species $[Na_2(H_2O)_2Fe_2(P_2W_{15}O_{56})_2]^{16-}$, the junctions between the trivacant moieties $\{P_2W_{15}\}$ and the metallic sheet are both of the α-type (Figure 2), whereas in the case of the trimetallic complexes ($M^{2+/3+}$ = Co^{2+} or Fe^{3+}), the structures may be considered as resulting from the fusion of one α-$\{M_3P_2W_{15}\}$ and one "lacunary" β-$\{M_2P_2W_{15}\}$ unit, and the lacuna is occupied by a Na^+ cation.[8–10]

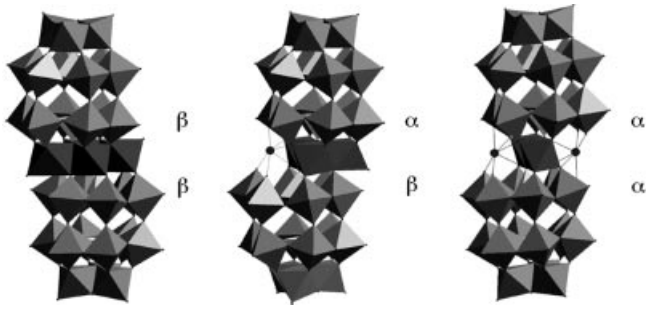

Figure 2. Polyhedral representations of the crystallographically resolved Dawson sandwich structures: ββ-$\{M_4P_4W_{30}\}$ (left), αβ-$\{NaM_3P_4W_{30}\}$ (middle) and αα-$\{Na_2M_2P_4W_{30}\}$ (right). For the "lacunary" structures, the aqua ligands are omitted for clarity.

As the Na^+ cations are weakly bonded, the di- and trimetallic complexes may act as divacant and monovacant "lacunary" species, respectively, and mixed-metal sandwich complexes can be obtained by addition of a transition-metal cation M^{n+}. Indeed, the reaction of M^{2+} (M = Mn, Co, Ni, Zn) with $\{Na_2Fe_2P_4W_{30}\}$ leads to "saturated" sandwich complexes $[M^{II}_2(H_2O)_2Fe^{III}_2(P_2W_{15}O_{56})_2]^{14-}$ (abbreviated as $\{M_2Fe_2P_4W_{30}\}$).[7b,11,12] In each case, replacement of the two Na^+ cations by two M^{2+} metallic cations induces conformational changes that lead to a β connectivity for both $\{P_2W_{15}\}$–M_2Fe_2 junctions.

The tricobalt species $[NaCo_3(H_2O)_2(P_2W_{15}O_{56})_2]^{17-}$ (abbreviated as $\{NaCo_3P_4W_{30}\}$)[8] reported recently also appears to be a suitable starting species for the synthesis of mixed-metal sandwich complexes (Figure 3).

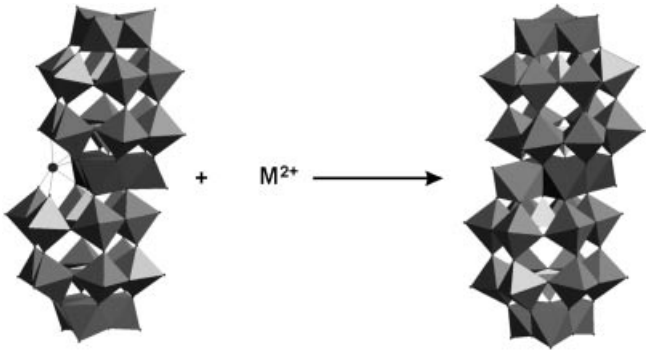

Figure 3. Principle of the synthesis of the mixed-metal Dawson sandwich complexes $\{MCo_3P_4W_{30}\}$.

Such complexes can be used in catalytic reactions as inorganic analogues of metalloporphyrins, and both the redox and the catalytic properties of these complexes can be modulated by the nature of the addendum atom M.[13]

We report here the synthesis and characterization (by IR and ^{31}P NMR spectroscopy and elemental analysis) of a new family of these mixed-metal sandwich complexes $[MCo_3(H_2O)_2(P_2W_{15}O_{56})_2]^{16-}$ (abbreviated as $\{MCo_3P_4W_{30}\}$) where M^{2+} = Mn^{2+}, Co^{2+}, Ni^{2+}, Zn^{2+} and Cd^{2+}. We also present the electrochemical behaviour of $\{MCo_3P_4W_{30}\}$ and compare it with that of the tetracobalt complex and the trinuclear precursor $\{NaCo_3P_4W_{30}\}$.[8]

Results and Discussion

Synthesis

The tricobalt sandwich complex is formally an unsaturated species. As shown by ^{31}P NMR spectroscopy, addition of a slight excess of Co^{2+} to the aqueous solution of $\{NaCo_3P_4W_{30}\}$ leads to the immediate and quantitative formation of one dissymmetrical $\{Co_4P_4W_{30}\}$ complex (Figure 4, middle)[8] according to the global reaction [Equation (1)]:

$$[NaCo_3(H_2O)_2(P_2W_{15}O_{56})_2]^{17-} + Co^{2+} \rightarrow \text{dissym-}[Co_4(H_2O)_2(P_2W_{15}O_{56})_2]^{16-} + Na^+ \quad (1)$$

The pH of the solution (initially around 6.5) does not change markedly by addition of Co^{2+}. At this pH, the dissymmetrical complex appears very stable, whereas at low pH (ca. 3) it evolves into the symmetrical ββ-$\{Co_4P_4W_{30}\}$ form (Figure 4, bottom).[15] As reported by Coronado and co-workers,[10] the lacunary $\{NaCo_3P_4W_{30}\}$ species presents an αβ connectivity; the rapid addition of Co^{2+} to form the saturated compound likely leads primarily to the αβ-$\{Co_4P_4W_{30}\}$ isomer, which is stable in neutral medium. In acidic medium, however, it isomerizes slowly and irreversibly into ββ-$\{Co_4P_4W_{30}\}$ by formal π/3-rotation of the $\{P_2W_{15}\}$ unit of the α-$\{Co_3P_2W_{15}\}$ moiety leading to β-$\{Co_3P_2W_{15}\}$. The whole process is described as follows [Equation (2)] and [Equation (3)]:

$$\alpha\beta\text{-}[NaCo_3(H_2O)_2(P_2W_{15}O_{56})_2]^{17-} + Co^{2+} \xrightarrow{\text{rapid, pH ca. 6.5}} \alpha\beta\text{-}[Co_4(H_2O)_2(P_2W_{15}O_{56})_2]^{16-} + Na^+ \quad (2)$$

$$\alpha\beta\text{-}[Co_4(H_2O)_2(P_2W_{15}O_{56})_2]^{16-} \xrightarrow{\text{slow, pH ca. 3}} \beta\beta\text{-}[Co_4(H_2O)_2(P_2W_{15}O_{56})_2]^{16-} \quad (3)$$

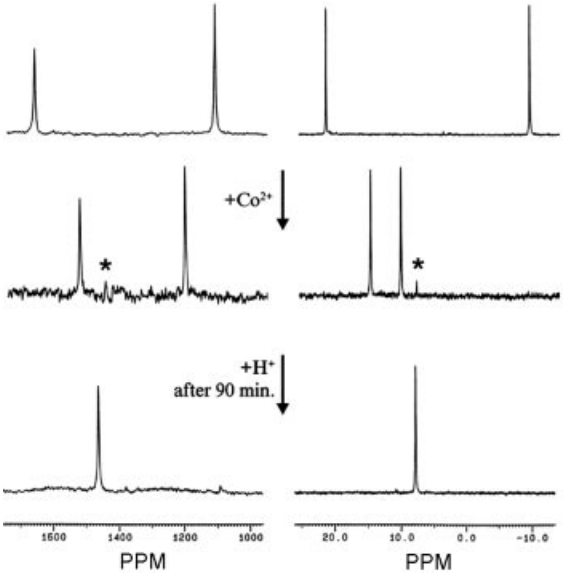

Figure 4. Formation of $\{CoCo_3P_4W_{30}\}$ by addition of Co^{2+} to $\{NaCo_3P_4W_{30}\}$ followed by 121.5 MHz ^{31}P NMR spectroscopy. Top: initial spectrum of $\{NaCo_3P_4W_{30}\}$, middle: immediately after addition of 2 equiv. Co^{2+} per $\{NaCo_3P_4W_{30}\}$, bottom: after lowering the pH by addition of 2 equiv. H_3O^+. Experimental conditions: c = 0.02 mol L^{-1} in D_2O/H_2O (1:1), T = 300 K.

To obtain analytically pure αβ-$Na_{16}[Co_4(H_2O)_2(P_2W_{15}O_{56})_2]$ it is necessary to use a fourfold excess of Co^{2+} in order to displace the Na^+ cation from the central $Na\text{-}Co_3O_{14}(H_2O)_2$ cluster. Actually, by using less than four equivalents of Co^{2+}, a mixture of αβ-$\{Co_4P_4W_{30}\}$ and αβ-$\{NaCo_3P_4W_{30}\}$ is always obtained. The crystallisation of $\{MCo_3P_4W_{30}\}$ further requires the addition of NaCl in order to lower the solubility by ionic strength and common cation effects.

The mixed-metal tricobalt sandwich complexes $\{MCo_3P_4W_{30}\}$ (M = Mn^{2+}, Ni^{2+}, Zn^{2+} and Cd^{2+}) are prepared similarly by addition of a fourfold excess of M^{2+} to $\{NaCo_3P_4W_{30}\}$ in 1 mol L^{-1} NaCl. ^{31}P NMR spectroscopy shows that the addition reaction is quite selective as no other compound can be detected except for trace amounts of the $\{NaCo_3P_4W_{30}\}$ precursor.

This method, namely simple addition of a transition-metal ion to the "lacunary" tricobalt compound, then leads to a clean reaction without any substitution in the POM subunits. This furnishes a coherent series of new mixed-metal sandwich complexes.

IR Characterization

The IR spectra of $\{MCo_3P_4W_{30}\}$ (M^{2+} = Mn^{2+}, Co^{2+}, Ni^{2+}, Zn^{2+} and Cd^{2+}) are shown in Figure S1 (see Supporting Information) and are compared to that of the precursor compound αβ-$\{NaCo_3P_4W_{30}\}$ and to that of ββ-$\{Co_4P_4W_{30}\}$.

In addition to numerous W–O and W–O–W bands at relatively low wavenumbers (<1000 cm^{-1}),[16] the IR spectra of phosphorus-centred polyoxotungstates present well-separated P–O stretching vibrations between 1200 and 1000 cm^{-1}.[17]

In our previous papers, we have discussed in detail the pattern of the PO_4 stretching region for various ββ-$\{M_4P_4W_{30}\}$ sandwich complexes; it shows two bands at around 1080 (strong) and 1010 cm^{-1} (weak) that are assigned to the unperturbed PW_9 moiety and one band at ca. 1055 cm^{-1} (medium) that is attributed to the perturbed PW_6 subunit.[7a,8] For the tricobalt precursor αβ-$\{NaCo_3P_4W_{30}\}$, the latter signal is split into two bands, at 1044 cm^{-1} and 1035 cm^{-1}, according to the non-equivalence of the two PW_6 subunits (PW_6Co_3 and PW_6Co_2Na).[8,10]

The mixed-tricobalt species $\{MCo_3P_4W_{30}\}$ can be formed from the trimetallic species by replacing the "external" Na^+ ion by one transition metal (Figure 3). Unlike those for $\{CdCo_3P_4W_{30}\}$, the two bands for the PW_6 subunits in $\{NaCo_3P_4W_{30}\}$ coalesce into one band at ca. 1050 cm^{-1}, which shows that the two saturated subunits PW_6Co_3 and PW_6Co_2M are nearly equivalent. Such a behaviour was already observed for lacunary and monosubstituted Keggin tungstophosphates, where addition of the transition-metal cation to the lacunary species induces a marked decrease in the splitting of the P–O stretching vibrations.[17a]

Whereas the size of the first row transition-metal cations Mn^{2+} (r = 0.83 Å), Ni^{2+}(r = 0.69 Å) and Zn^{2+} (r = 0.74 Å) are comparable to that of Co^{2+} (r = 0.74 Å), the cadmium cation is significantly larger (r = 0.95 Å) and it does not fit exactly into the lacuna and therefore does not interact as strongly as the other cations with the oxygen atom of PO_4. This accounts for the observation of two bands at around 1045 cm^{-1} (PW_6Co_3) and 1035 cm^{-1} (shoulder, PW_6Co_2Cd) for $\{CdCo_3P_4W_{30}\}$. Nevertheless, the overall IR spectra of all $\{MCo_3P_4W_{30}\}$ are similar to that of $\{Co_4P_4W_{30}\}$, which indicates a structural similarity throughout the whole series.

^{31}P NMR Characterization

^{31}P NMR spectroscopy is particularly suitable to check the polyoxometalate purity and to obtain some structural information, i.e. overall symmetry of the species and relative positions of the substituting elements.[12]

The ^{31}P NMR spectra of $\{MCo_3P_4W_{30}\}$ (M^{2+} = Mn^{2+}, Co^{2+}, Ni^{2+}, Zn^{2+} and Cd^{2+}) are reported in Figure 5 and all data are given in Table 1. Paramagnetic Dawson species always exhibit two markedly different types of ^{31}P resonances: the P atoms labelled P(1) in the PW_6 subunits close to the paramagnetic centres give rise to broad and strongly shifted (generally towards high frequency) signals, and those labelled P(2) in the PW_9 subunits far from the paramagnetic centres give rise to relatively sharp lines at a chemical shift close to that of diamagnetic metallophosphates (between +20 and –20 ppm).[18]

As in the case for $\{NaCo_3P_4W_{30}\}$, the ^{31}P NMR spectra of all $\{MCo_3P_4W_{30}\}$ present two relatively narrow lines ($\Delta\nu_{1/2}$: 10–30 Hz) of equal intensity, which are assigned to

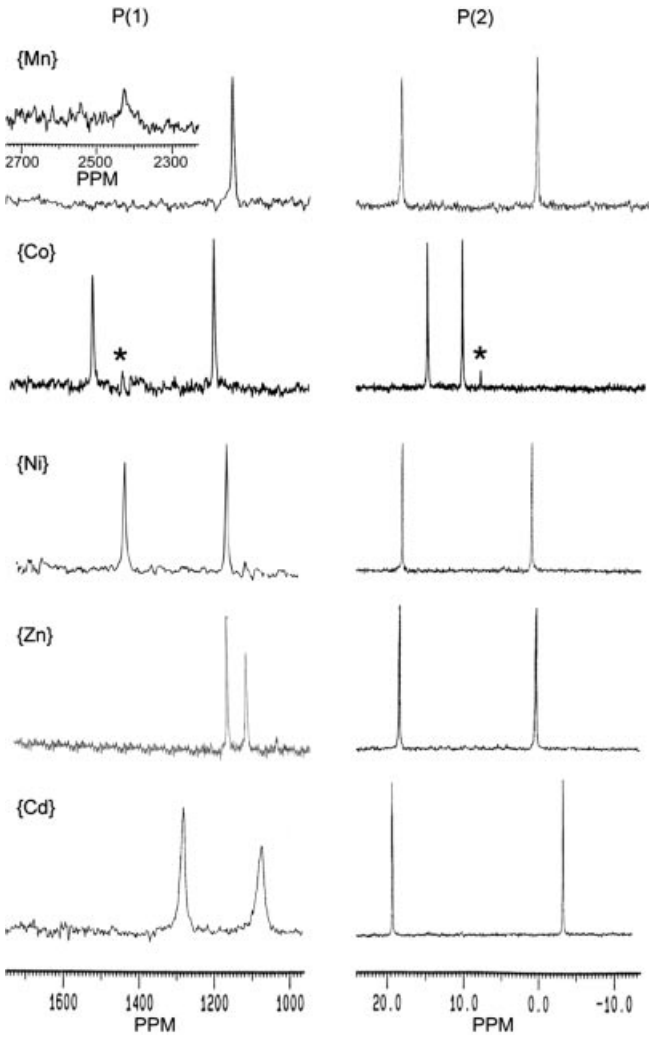

Figure 5. 121.5 MHz ^{31}P NMR spectra of various $\{MCo_3P_4W_{30}\}$ [0.02 mol L^{-1} in unbuffered solutions in D_2O/H_2O (1:1)] (from top to bottom: M^{2+} = Mn^{2+}, Co^{2+}, Ni^{2+}, Zn^{2+} and Cd^{2+}).

Table 1. ^{31}P NMR spectroscopic data for the Dawson sandwich species.[a]

Compound	P(1)[b]		P(2)[b]	
	δ[c]	$\Delta\nu_{1/2}$[d]	δ[c]	$\Delta\nu_{1/2}$[d]
ββ-$\{Co_4P_4W_{30}\}$	+1483	420	+9.9	20
αβ-$\{NaCo_3P_4W_{30}\}$	+1125	450	–9.3	10
	+1673	450	+22.0	10
$\{MnCo_3P_4W_{30}\}$	+1150	470	+0.4	17
	+2425	2400	+18.4	21
$\{CoCo_3P_4W_{30}\}$	+1203	440	+10.0	14
	+1522	540	+14.5	13
$\{NiCo_3P_4W_{30}\}$	+1164	450	+0.6	31
	+1435	630	+17.9	31
$\{ZnCo_3P_4W_{30}\}$	+1163	550	+0.4	10
	+1116	365	+18.4	10
$\{CdCo_3P_4W_{30}\}$	+1075	250	–3.2	8
	+1283	430	+19.2	8

[a] Unbuffered 0.02 mol L^{-1} solutions in D_2O/H_2O (1:1) at 300 K. [b] P(1) and P(2) in the PW_6 and PW_9 subunits, respectively. [c] In ppm with respect to 85% H_3PO_4. [d] In Hz.

the two non-equivalent P(2) atoms, and two broad signals attributed to the P(1) atoms (Figure 5). This confirms that the two $\{P_2W_{15}\}$ moieties remain non-equivalent in the $\{MCo_3P_4W_{30}\}$ complexes (Figure 3).

By examination of the data reported in Table 1, we notice that, for all first-row transition-metal species, one P(1) signal is always observed from about +1150 to +1200 ppm. By plotting its ^{31}P chemical shift with respect to the atomic number of M^{2+}, we observe a moderate and quasilinear variation, whereas the second P(1) signal shifts considerably (Figure 6a). We can tentatively assign the latter signal to the P(1) atom of the PW_6Co_2M subunit that is closer to the addendum M^{2+} cation ($d_{P(1)-M}$: ca. 3.3 Å) rather than to the P(1) atom of the PW_6Co_3 subunit ($d_{P(1)-M}$: ca. 4.6 Å). On the contrary, the P(2) chemical shifts are not very sensitive to the nature of M^{2+} with the exception of Co^{2+}. Two P(2) signals are observed at around +0.4 to +0.6 ppm and +17.9 to +18.4 ppm, which agrees with phosphorus atoms in the PW_9 subunits far from the paramagnetic centres ($d_{P(2)-M} > 7$ Å) and consequently less affected (Figure 6b). It is somewhat puzzling that both the P(2) chemical shifts

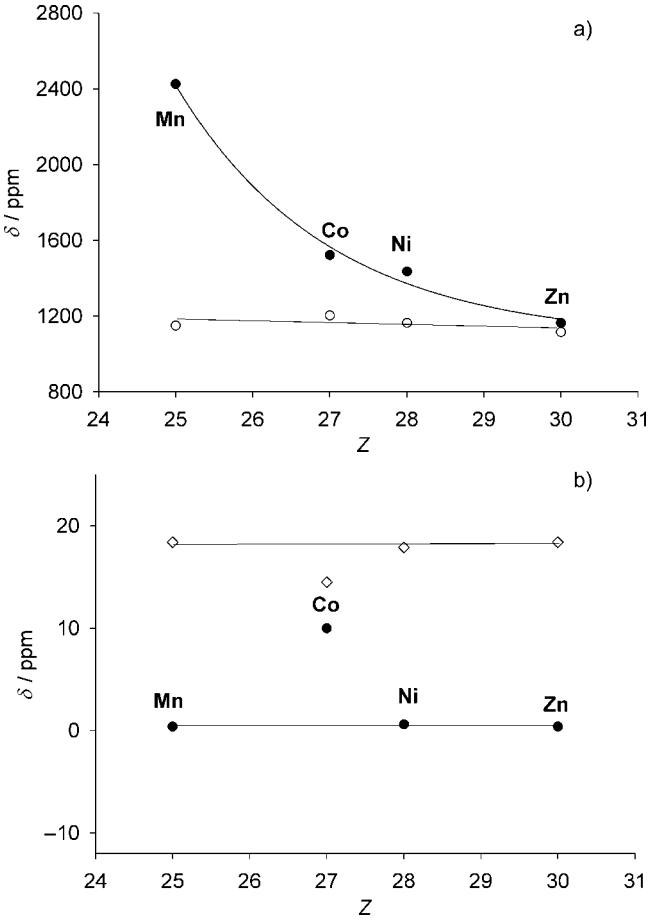

Figure 6. Plot of the variation of a) $\delta_{P(1)}$ and b) $\delta_{P(2)}$ of $\{MCo_3P_4W_{30}\}$ (M^{2+} = Mn^{2+}, Co^{2+}, Ni^{2+} and Zn^{2+}) with respect to the atomic number of M. (For the complete series including Cd^{2+} see Figure S3 of the Supporting Information).

for αβ-$\{Co_4P_4W_{30}\}$ do not fall on the line, which may suggest that the $\{MCo_3P_4W_{30}\}$ (M ≠ Co) species present another conformation with ββ connectivities. This question cannot be answered until an X-ray structure determination has been performed.

We notice that the Mn compound presents the largest shift amongst the P(1) signals (+2425 ppm); this ^{31}P resonance is also the broadest one (2.4 kHz, Figure 5, top).

Electrochemistry

General Electrochemical Behaviour

The electrochemical behaviour of complexes $\{NaCo_3P_4W_{30}\}$ and $\{MCo_3P_4W_{30}\}$ was studied in aqueous solution (pH 3.5) by cyclic voltammetry (CV). All electrochemical data are gathered in Table 2, and typical cyclic voltammograms are presented in Figure 7 and Figure 8.

These complexes exhibit three successive reduction processes involving the W centres. For these three couples, the cathodic (and anodic) peak currents are almost proportional to the square root of the scan rate up to 100 mV s^{-1}, which indicates that the reduction (and oxidation) processes are both diffusion-controlled.

The voltammograms of $\{ZnCo_3P_4W_{30}\}$, $\{NiCo_3P_4W_{30}\}$ and αβ-$\{Co_4P_4W_{30}\}$ are very similar to that of ββ-$\{Co_4P_4W_{30}\}$ (Figure 7 top and Figure S2), however, with slightly different potentials (Table 2).

In the case of $\{CdCo_3P_4W_{30}\}$, the third reduction process presents a typical pattern that is characteristic of adsorption of metallic Cd at the electrode (Figure 7, bottom). In the forward scan, at –0.859 V, Cd^{2+} is also reduced along with the W centres; this results in the deposition of metallic Cd. In the reverse scan, Cd^0 is reoxidized to Cd^{2+}, which re-enters the sandwich anion; this gives rise to the intense and symmetrical anodic redissolution peak. The whole reduction and the first reoxidation processes of $\{CdCo_3P_4W_{30}\}$ can be expressed according to Equations (4), (5), (6), (7) and (8).

For all species, controlled-potential coulometry at –0.55 V shows that the solution turns deep blue and consumes between 2.1 and 2.2 electrons per sandwich complex;

$$[CdCo_3(H_2O)_2(P_2W_{15}O_{56})_2]^{16-} + 2e^- \leftrightarrows [CdCo_3(H_2O)_2(P_2W_{15}O_{56})_2]^{18-} \quad (4)$$

$$[CdCo_3(H_2O)_2(P_2W_{15}O_{56})_2]^{18-} + 2e^- \leftrightarrows [CdCo_3(H_2O)_2(P_2W_{15}O_{56})_2]^{20-} \quad (5)$$

$$[CdCo_3(H_2O)_2(P_2W_{15}O_{56})_2]^{20-} + 4e^- + Na^+ \rightarrow [NaCo_3(H_2O)_2(P_2W_{15}O_{56})_2]^{23-} + Cd^0 \quad (6)$$

$$Cd^0 \rightarrow Cd^{2+} + 2e^- \quad (7)$$

$$[NaCo_3(H_2O)_2(P_2W_{15}O_{56})_2]^{23-} + Cd^{2+} \rightarrow [CdCo_3(H_2O)_2(P_2W_{15}O_{56})_2]^{20-} + 2e^- + Na^+ \quad (8)$$

at –0.70 V, the number of exchanged electrons is between 4.1 and 4.3. This shows that both the first and the second processes involve two electrons.

In addition to the cathodic waves as discussed above, the manganese species $\{MnCo_3P_4W_{30}\}$ is also electroactive at a positive potential: an anodic peak at +1.027 V and the associated cathodic peak at +0.719 V correspond to the oxidation and reduction of the Mn centre (Figure 8).[7a,12,19]

Controlled-potential coulometry at +1.10 V results in the passage of 2.2 electrons per complex, whereas subsequent reduction at +0.60 V consumes only 1.1 electron. This suggests that the Mn^{II} is oxidized directly to Mn^{IV}, but in the reverse process Mn^{IV} is reduced to Mn^{III}; further reduction to recover Mn^{II} in $\{MnCo_3P_4W_{30}\}$ likely leads to a broad peak hardly detectable even after several repetitive scans.

Similar behaviours were previously reported for α$_2$-$[Mn^{II}P_2W_{17}O_{61}]^{8-}$, $[ZnW_{11}MnO_{39}]^{8-}$ and $[Mn_4(H_2O)_2(P_2W_{15}O_{56})_2]^{16-}$ (abbreviated as $\{Mn_4P_4W_{30}\}$); in the last case, the four Mn centres are simultaneously oxidized in a eight-electron process, and the two successive reduction processes Mn^{IV} to Mn^{III} and Mn^{III} to Mn^{II} both consume four electrons.[7a,19]

In that case, the curve-crossing at about 1 V is probably due to the deposition, at the electrode, of the species generated during the oxidation process (Figure 8, dotted line).

Table 2. Electrochemical data of the Dawson sandwich complexes obtained from cyclic voltammetry (scan rate = 20 mV s^{-1}) in 0.5 mol L^{-1} Na_2SO_4 + H_2SO_4 (pH 3.5). All redox potentials $E°'$, approximated by $(E_p^a + E_p^c)/2$ for the reversible steps, are given in V vs. SCE.

Compound	W(1)[a]	W(2)[a]	W(3)[a]	Mn
ββ-$\{Co_4P_4W_{30}\}$	–0.436 (2e, 71)	–0.641 (2e, 144)	–0.832 (1e, 64) –0.917 (1e, 94)	
αβ-$\{NaCo_3P_4W_{30}\}$	–0.470 (1e, 93)[b] –0.531 (1e, 58)[b]	–0.660 (2e, 83)[c]	–0.835 (2e, 65)[c]	
$\{MnCo_3P_4W_{30}\}$	–0.482 (2e, 106)	–0.673 (2e, 124)	–0.908 (2e, 84)	E_p^a = +1.027 E_p^c = +0.719
$\{CoCo_3P_4W_{30}\}$	–0.467 (2e, 126)	–0.673 (2e, 114)	–0.903 (2e, 110)	
$\{NiCo_3P_4W_{30}\}$	–0.470 (2e, 121)	–0.663 (2e, 116)	–0.896 (2e, 100)	
$\{ZnCo_3P_4W_{30}\}$	–0.465 (2e, 121)	–0.690 (2e, 81)	–0.909 (2e, 101)	
$\{CdCo_3P_4W_{30}\}$	–0.488 (2e, 128)	–0.693 (2e, 151)	–0.859 (4e, 225)[d]	

[a] In parentheses: number of exchanged electron(s) n and $\Delta E_p = |E_p^a - E_p^c|$. [b] Simultaneous exchange of one electron and one proton (see ref.[7a]). [c] Simultaneous exchange of two electrons and two protons (see ref.[7a]). [d] Irreversible, see text.

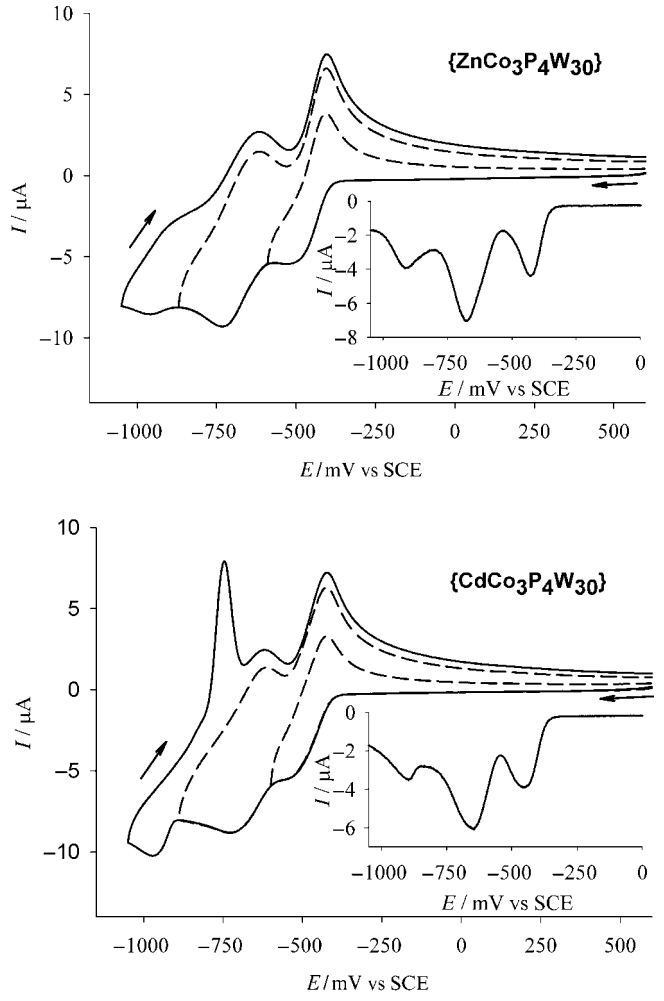

Figure 7. Cyclic voltammograms of $\{ZnCo_3P_4W_{30}\}$ (top) and $\{CdCo_3P_4W_{30}\}$ (bottom) in 0.5 mol L^{-1} Na_2SO_4 + H_2SO_4 at pH 3.5 with different negative potential limits: –0.60 V, –0.89 V and –1.05 V. Scan rate = 20 mV s^{-1}, c = 0.5 mmol L^{-1}. Inset: Differential pulse voltammetry at a scan rate of 25 mV s^{-1}.

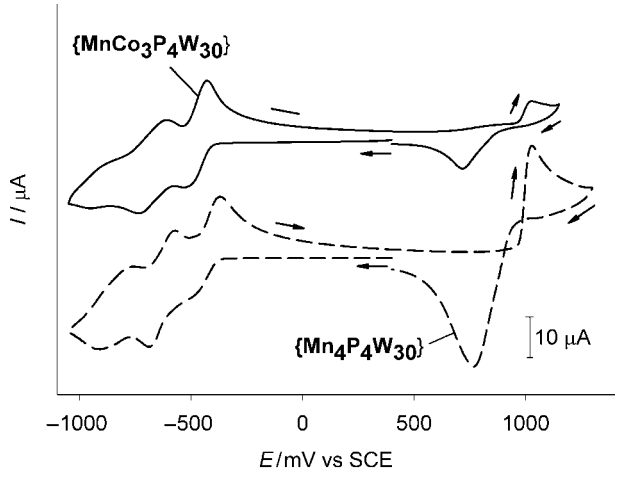

Figure 8. Cyclic voltammograms of $\{MnCo_3P_4W_{30}\}$ (full line) and $\{Mn_4P_4W_{30}\}$ (dotted line) in 0.5 mol L^{-1} Na_2SO_4 + H_2SO_4 at pH 3.5. Scan rate = 20 mV s^{-1}, c = 0.5 mmol L^{-1}.

Summary and Concluding Remarks

In this work, we report for the first time the preparation and characterization of mixed-metal–tricobalt sandwich complexes $[MCo_3(H_2O)_2(P_2W_{15}O_{56})_2]^{16-}$ ($\{MCo_3P_4W_{30}\}$; M^{2+} = Mn^{2+}, Co^{2+}, Ni^{2+}, Zn^{2+} and Cd^{2+}).

As in the case for $\{NaCo_3P_4W_{30}\}$, the ^{31}P NMR spectrum of each $\{MCo_3P_4W_{30}\}$ complex presents two relatively narrow lines of equal intensity assigned to the two non-equivalent P(2) atoms and two broad signals attributed to the P(1) atoms, which indicates that the two $\{P_2W_{15}\}$ moieties remain non-equivalent in the $\{MCo_3P_4W_{30}\}$ complexes. Moreover, by plotting $\delta_{P(1)}$ with respect to the atomic number of M, we notice that one of the two P(1) signals presents a moderate and quasilinear shift with respect to the atomic number, whereas the second P(1) signal changes considerably. This large variation leads us to tentatively assign this signal to the P(1) atom of the PW_6Co_2M subunit that is closer to the addendum M^{2+} cation.

On the contrary, the P(2) signals are not very sensitive to the nature of M^{2+} (with the exception of Co^{2+}), which is in agreement with the fact that these phosphorus atoms are in the PW_9 subunits far from M^{2+}.

The electrochemical behaviours of $\{MCo_3P_4W_{30}\}$ were investigated systematically, with reference to that of αβ-$\{NaCo_3P_4W_{30}\}$ or ββ-$\{Co_4P_4W_{30}\}$. All these compounds exhibit three reversible W-centred reduction processes with slightly different peak potentials, which suggests that the anions have similar structures.

Different electrochemical behaviours can be distinguished: with Co^{2+}, Ni^{2+} and Zn^{2+}, the metallic centres are not electroactive, whereas with Mn^{2+} and Cd^{2+}, redox reactions originating from the metals are observed.

The Mn^{2+} complex presents one oxidation process, corresponding to the Mn^{II}/Mn^{IV} couple, followed, in the reverse scan, by the reduction of Mn^{IV} to Mn^{III}. Further reduction to recover Mn^{II} complex is hardly detectable.

The "lacunary" sandwich complex $\{NaCo_3P_4W_{30}\}$ appears to be a good precursor to prepare new classes of mixed-metal polytungstates in which the nature of the metal can be varied considerably. This opens the route to the preparation of mixed-metal sandwich complexes with interesting catalytic and magnetic properties.

Experimental Section

General Comment: Most common laboratory chemicals were of reagent grade purchased from commercial sources, and were used without further purification.

Preparation of Compounds: The trinuclear complex αβ-$[NaCo_3(H_2O)_2(P_2W_{15}O_{56})_2]^{17-}$ $\{NaCo_3P_4W_{30}\}$ was prepared as described previously.[8]

For all subsequent compounds, the purity was checked by ^{31}P NMR spectroscopy: except for $\{CoCo_3P_4W_{30}\}$, no spurious signal could be detected from the noise for all compounds, which shows that the purity is at least 97%.

αβ-$Na_{16}[Co_4(H_2O)_2(P_2W_{15}O_{56})_2]\cdot 51H_2O$: $\{NaCo_3P_4W_{30}\}$ (1.00 g, 0.110 mmol) was dissolved in 10 mL of water. By addition of

$Co(NO_3)_2{\cdot}6H_2O$ (128.0 mg, 0.440 mmol) while stirring vigorously, the solution immediately turned from dark red to brown. The resulting neutral solution (pH ca. 6.5) was stirred for 2 h, after which NaCl (0.60 g) was added. The solution was concentrated in air in an open vessel, and a greenish brown precipitate appeared after ca. 1 d. The precipitate was collected on a sintered glass frit (porosity 4) after 2 d and dried in air (yield 0.43 g, 43%). ^{31}P NMR spectroscopy shows that this sample is contaminated by less than 5% of the symmetrical ββ isomer. $Co_4Na_{16}P_4W_{30}O_{112}{\cdot}53H_2O$ (8989.7): calcd. Co 2.62, P 1.38, W 61.35, H_2O 10.62; found Co 2.60, P 1.38, W 61.21, H_2O 10.62. ^{31}P NMR: (D_2O/H_2O, 1:1): δ = +10.0 ($\Delta\nu_{1/2}$ = 14 Hz), +14.5 ($\Delta\nu_{1/2}$ = 13 Hz), +1203 ($\Delta\nu_{1/2}$ = 440 Hz), +1522 ppm ($\Delta\nu_{1/2}$ = 540 Hz).

$Na_{16}[MnCo_3(H_2O)_2(P_2W_{15}O_{56})_2]{\cdot}51H_2O$.: This complex was prepared following the same procedure as that for αβ-$\{Co_4P_4W_{30}\}$ by using $MnCl_2{\cdot}6H_2O$ (102.9 mg, 0.440 mmol) instead of $Co(NO_3)_2{\cdot}6H_2O$. The greenish-orange precipitate was collected on a sintered glass frit (porosity 4) after 2 d (yield 0.72 g, 73%). $MnCo_3Na_{16}P_4W_{30}O_{112}{\cdot}53H_2O$ (8985.7): calcd. Co 1.97, Mn 0.61, P 1.38, W 61.38, H_2O 10.63; found Co 1.95, Mn 0.63, P 1.37, W 61.29, H_2O 10.63. ^{31}P NMR: (D_2O/H_2O, 1:1), δ = +0.4 ($\Delta\nu_{1/2}$ = 17 Hz), +18.4 ($\Delta\nu_{1/2}$ = 21 Hz), +1150 ($\Delta\nu_{1/2}$ = 470 Hz), +2425 ppm ($\Delta\nu_{1/2}$ = 2.4 kHz).

$Na_{16}[NiCo_3(H_2O)_2(P_2W_{15}O_{56})_2]{\cdot}49H_2O$: This complex was prepared following the same procedure as that for αβ-$\{Co_4P_4W_{30}\}$ by using $NiCl_2{\cdot}6H_2O$ (104.4 mg, 0.440 mmol) instead of $Co(NO_3)_2{\cdot}6H_2O$. The yellow-brown precipitate was collected on a sintered glass frit (porosity 4) after 2 d (yield 0.68 g, 69%). $NiCo_3Na_{16}P_4W_{30}O_{112}{\cdot}51H_2O$ (8989.5): calcd. Co 1.97, Ni 0.66, P 1.38, W 61.60, H_2O 10.26; found Co 1.99, Ni 0.63, P 1.39, W 61.70, H_2O 10.26. ^{31}P NMR: (D_2O/H_2O, 1:1): δ = +0.6 ($\Delta\nu_{1/2}$ = 31 Hz), +17.9 ($\Delta\nu_{1/2}$ = 31 Hz), +1164 ($\Delta\nu_{1/2}$ = 450 Hz), +1435 ($\Delta\nu_{1/2}$ = 630 Hz).

$Na_{16}[ZnCo_3(H_2O)_2(P_2W_{15}O_{56})_2]{\cdot}49H_2O$: This complex was prepared following the same procedure as that for αβ-$\{Co_4P_4W_{30}\}$ by using $ZnCl_2{\cdot}6H_2O$ (107.5 mg, 0.440 mmol) instead of $Co(NO_3)_2{\cdot}6H_2O$. The grey-brown precipitate was collected on a sintered glass frit (porosity 4) after 2 d (yield 0.84 g, 85%). $ZnCo_3Na_{16}P_4W_{30}O_{112}{\cdot}51H_2O$ (8996.1): calcd. Co 1.97, P 1.38, W 61.56, Zn 0.73, H_2O 10.25; found Co 1.96, P 1.35, W 61.91, Zn 0.76, H_2O 10.25. ^{31}P NMR: (D_2O/H_2O, 1:1): δ = +0.4 ($\Delta\nu_{1/2}$ = 10 Hz), +18.4 ppm ($\Delta\nu_{1/2}$ = 10 Hz), +1116 ppm ($\Delta\nu_{1/2}$ = 365 Hz), +1163 ($\Delta\nu_{1/2}$ = 550 Hz).

$Na_{16}[CdCo_3(H_2O)_2(P_2W_{15}O_{56})_2]{\cdot}47H_2O$: This complex was prepared following the same procedure as that for αβ-$\{Co_4P_4W_{30}\}$ by using $CdCl_2{\cdot}6H_2O$ (128.0 mg, 0.440 mmol) instead of $Co(NO_3)_2{\cdot}6H_2O$. The grey-brown precipitate was collected on a sintered glass frit (porosity 4) after 2 d (yield 0.70 g, 71%). $CdCo_3Na_{16}P_4W_{30}O_{112}{\cdot}49H_2O$ (9043.2): calcd. Cd 1.25, Co 1.97, P 1.38, W 61.48, H_2O 9.84; found Cd 1.22, Co 1.94, P 1.39, W 61.24, H_2O 9.84. ^{31}P NMR: (D_2O/H_2O, 1:1): δ = –3.2 ($\Delta\nu_{1/2}$ = 8 Hz), +19.2 ($\Delta\nu_{1/2}$ = 8 Hz), +1075 ($\Delta\nu_{1/2}$ = 250 Hz), +1283 ppm ($\Delta\nu_{1/2}$ = 430 Hz).

NMR and IR Spectroscopic Measurements: ^{31}P NMR spectra were recorded in 5-mm o.d. tubes on a Bruker AC 300 or a Bruker AvanceII 300 spectrometer operating at 121.5 MHz. The NMR spectra were obtained at 300 K with 0.02 M solutions in D_2O/H_2O (1:1) and were referenced to external 85% H_3PO_4 (IUPAC convention) by the substitution method. The ^{31}P chemical shifts are pH dependent and some small differences may be observed between the synthetic solution and those obtained after redissolving the solid samples. IR spectra were recorded on a Bio-Rad FTS 165 FTIR spectrophotometer on KBr pellets.

Electrochemical Experiments: Water, used for all electrochemical measurements, was obtained by passing through a Milli-RO_4 unit and subsequently through a Millipore Q water purification set. H_2SO_4 solutions and solid Na_2SO_4 were commercial products (Prolabo). The electrolyte was made up from 0.5 M Na_2SO_4 aqueous solution, and its pH was precisely adjusted to 3.5 by addition of 0.5 M (H_2SO_4 + Na_2SO_4) aqueous solution. The solutions were deaerated thoroughly for at least 30 min by bubbling argon (Ar-U from Air Liquide) through the solution and kept under argon atmosphere during the whole experiment.

The source, mounting and polishing of the glassy carbon electrode (GC, Tokai, Japan) have been described previously.[14] The glassy carbon samples had a diameter of 3 mm. The electrochemical apparatus EG&G 273A was driven by a personal computer. Potentials are quoted against a saturated calomel electrode (SCE). The counter electrode was a platinum gauze with a large surface area. All experiments were carried out at room temperature. Controlled potential coulometry experiments were conducted under continuous bubbling and stirring, and a large surface glassy carbon plate (s = 6 cm^2) was used.

Analyses: Elemental analyses were performed by the Service Central d'Analyse du CNRS, Vernaison (France). The water content was determined by thermogravimetric analysis.

Supporting Information (see footnote on the first page of this article): The IR spectra of $\{MCo_3P_4W_{30}\}$ (Figure S1), cyclic voltammograms of ββ-$\{Co_4P_4W_{30}\}$ and αβ-$\{Co_4P_4W_{30}\}$ at pH 3.5 (Figure S2) and plot of the variation of $\delta_{P(1)}$ and $\delta_{P(2)}$ of $\{MCo_3P_4W_{30}\}$, including that of M = Cd^{2+} (Figure S3).

Acknowledgments

This work was supported by the CNRS and by the Université Paris-Sud 11 and Université Pierre et Marie Curie – Paris6. This work was also supported by the ANR agency, project no. JC05_52436, NCPPOM.

[1] E. Coronado, C. J. Gómez-García, *Chem. Rev.* **1998**, *98*, 273.
[2] M. T. Pope, A. Müller (Eds.), Polyoxometalates: *From Platonic Solids to Anti-Retroviral Activity*, Kluwer, Dordrecht, The Netherlands, **1994**.
[3] J. T. Rhule, C. L. Hill, D. A. Judd, R. F. Schinazi, *Chem. Rev.* **1998**, *98*, 327.
[4] I. V. Kozhevnikov, *Chem. Rev.* **1998**, *98*, 171.
[5] a) R. G. Finke, M. W. Droege, *Inorg. Chem.* **1983**, *22*, 1006; b) R. G. Finke, M. W. Droege, P. J. Domaille, *Inorg. Chem.* **1987**, *26*, 3886; c) T. J. R. Weakley, R. G. Finke, *Inorg. Chem.* **1990**, *29*, 1235; d) J.-P. Ciabrini, R. Contant, *J. Chem. Res.* **1993**, *(S)* 391, *(M)* 2719; e) C. J. Gómez-García, J. J. Borrás-Almenar, E. Coronado, L. Ouahab, *Inorg. Chem.* **1994**, *33*, 4016; f) R. G. Finke, T. J. R. Weakley, *J. Chem. Crystallogr.* **1994**, *24*, 123; g) J. F. Kirby, L. C. W. Baker, *J. Am. Chem. Soc.* **1995**, *117*, 10010; h) X. Zhang, D. C. Duncan, C. F. Campana, C. L. Hill, *Inorg. Chem.* **1997**, *36*, 4208; i) A. Müller, F. Peter, M. Pope, D. Gatteschi, *Chem. Rev.* **1998**, *98*, 239; j) L. Meng, J. F. Liu, *Chem. Res. Chin. Univ.* **1998**, *14*, 1.
[6] R. Thouvenot, M. Fournier, R. Franck, C. Rocchiccioli-Deltcheff, *Inorg. Chem.* **1984**, *23*, 598–605.
[7] a) L. Ruhlmann, L. Nadjo, J. Canny, R. Contant, R. Thouvenot, *Eur. J. Inorg. Chem.* **2002**, 975–986; b) X. Zhang, C. L. Hill, *Chem. Ind.* **1998**, *75*, 519; c) X. Zhang, T. M. Anderson, Q. Chen, C. L. Hill, *Inorg. Chem.* **2001**, *40*, 418–419.

[8] L. Ruhlmann, J. Canny, R. Contant, R. Thouvenot, *Inorg. Chem.* **2002**, *41*, 3811–3819.
[9] a) T. M. Anderson, K. I. Hardcastle, N. Okun, C. L. Hill, *Inorg. Chem.* **2001**, *40*, 6418; b) I. M. Mbomekalle, B. Keita, L. Nadjo, W. A. Neiwert, L. Zhang, K. I. Hardcastle, C. L. Hill, T. M. Anderson, *Eur. J. Inorg. Chem.* **2003**, 3924–3928; c) B. Keita, I. M. Mbomekalle, L. Nadjo, T. M. Anderson, C. L. Hill, *Inorg. Chem.* **2004**, *43*, 3257–3263.
[10] J. M. Clemente-Juan, E. Coronado, A. Gaita-Ariño, C. Giménez-Saiz, H.-U. Gu1del, A. Sieber, R. Bircher, H. Mutka, *Inorg. Chem.* **2005**, *44*, 3389–3395.
[11] a) T. M. Anderson, X. Zhang, K. I. Hardcastle, C. L. Hill, *Inorg. Chem.* **2002**, *41*, 2477; b) I. M. Mbomekalle, R. Cao, K. I. Hardcaste, C. L. Hill, M. Amman, B. Keita, L. Nadjo, T. M. Anderson, *C R. Chimie* **2005**, *8*, 1077–1086.
[12] L. Ruhlmann, J. Canny, J. Vaisserman, R. Thouvenot, *Dalton Trans.* **2004**, *5*, 794–800.
[13] a) L. C. W. Baker, Plenary Lecture, Proc. XV International Conference Coordination Chemistry 15th, **1973**; b) D. K. Lyon, W. K. Miller, T. Novet, P. J. Domaille, E. Evitt, D. C. Johnson, R. G. Finke, *J. Am. Chem. Soc.* **1991**, *113*, 7209–7221.
[14] B. Keita, K. Essaadi, L. Nadjo, *J. Electroanal. Chem. Interfacial. Electrochem.* **1989**, *259*, 127–146.
[15] The X-ray structure of ββ-$Na_{16}[Co_4(H_2O)_2(P_2W_{15}O_{56})_2]\cdot 51H_2O$ has been reported in detail recently. The anion $[Co_4(H_2O)_2(P_2W_{15}O_{56})_2]^{16-}$ contains a sheet of four Co^{II} ions forming an oxo–aqua metallic core $Co_4O_{14}(H_2O)_2$, which is sandwiched between two trivacant α-$[P_2W_{15}O_{56}]^{12-}$ ({P_2W_{15}}) subunits, with two β connectivities. The crystal structure confirms the C_{2h} symmetry of the whole polyanion, which is in agreement with ^{31}P NMR spectroscopy. S. Liu, D. G. Kurth, B. Bredenkőtter, D. Volkmer, *J. Am. Chem. Soc.* **2002**, *124*, 12279–12287.
[16] C. Rocchiccioli-Deltcheff, R. Thouvenot, R. Franck, *Spectrochim. Acta* **1976**, *22A*, 587–597.
[17] a) C. Rocchiccioli-Deltcheff, R. Thouvenot, *J. Chem. Res.* **1977**, *(S)* 46–47, *(M)* 549–571; b) C. Rocchiccioli-Deltcheff, R. Thouvenot, *Spectroscopy Letters* **1979**, *12*, 127–138.
[18] T. L. Jorris, M. Kozik, N. Casañ-Pastor, P. J. Domaille, R. G. Finke, W. K. Miller, L. C. W. Baker, *J. Am. Chem. Soc.* **1987**, *109*, 7402–7408.
[19] L. Cheng, H. Seen, J. Liu, S. Dong, *J. Chem. Soc., Dalton Trans.* **1999**, 2619–2625.

Received: October 5, 2006
Published Online: January 23, 2007

